Functional Ecology Volume 24 • Number 4 • August 2010

Cover image: A small sample of species illustrating the morphological diversity of neotropical leaf-nosed bats. Santana, Dumont & Davis (p. 776) investigated the mechanism of bite force production in these bats and its association with diet. Photo by Sharlene E. Santana.

WILEY-BLACKWELL

COPE COMMITTEE ON PUBLICATION ETHICS

Information on this journal can be accessed at **http://www.functionalecology.org**

Web based system for submission and review at **http://mc.manuscriptcentral.com/fe-besjournals**

This journal is a member of and subscribes to the principles of the Committee on Publication Ethics

This journal is available online at Wiley InterScience. Visit www3.interscience.wiley.com to search the articles and register for table of contents email alerts.

Typeset by SPS, India.
Printed in Singapore by KHL Printing Co Pte Ltd

Functional Ecology

Volume 24 • Number 4 • August 2010 • Pages 701–946

Functional Ecology

Volume 24 • Number 4 • August 2010

ISSN 0269-8463 (Print)
ISSN 1365-2435 (Online)

Editors: C. Fox, K. Thompson, F. Messina

- **Rethinking the value of high wood density**
- **The aerodynamics and efficiency of wind pollination**
- **What drives retrogressive succession?**
- **Parasites cause selection against migrants**

British Ecological Society

Functional Ecology

British Ecological Society

Functional Ecology 2010, **24**, 776–784 doi: 10.1111/j.1365-2435.2010.01703.x

Mechanics of bite force production and its relationship to diet in bats

Sharlene E. Santana*[,1], Elizabeth R. Dumont[2] and Julian L. Davis[3]

[1]*Graduate Program in Organismic and Evolutionary Biology, University of Massachusetts Amherst, Amherst, Massachusetts 01003, USA;* [2]*Biology Department, University of Massachusetts Amherst, Amherst, Massachusetts 01003, USA; and* [3]*Department of Mechanical and Industrial Engineering, University of Massachusetts Amherst, Amherst, Massachusetts 01003, USA*

Summary

1. In vertebrates, bite force is a measure of whole organism performance that is associated with both cranial morphology and dietary ecology. Mechanistic studies of bite force production have identified morphological features associated with bite force, and linked bite force with diet, but this approach has rarely been used in mammals.

2. Mammals are a good system with which to investigate the function of the feeding apparatus because of the relative simplicity of their skulls and their high dietary diversity. Phyllostomid bats are one of the most trophically and morphologically diverse groups of mammals, but we know little about the relative importance of biomechanical variables in producing bite force or how these variables vary with diet.

3. We combined *in vivo* measurements of bite force with assessments of muscular and bony morphology to build and validate a model describing the mechanics of bite force production in 25 species of bats. We used this model to investigate how bats with different diets vary in biomechanical parameters that contribute to bite force. In addition to traditional dietary categories, we used a functional definition of diet that reflects the mechanical demands (hardness) of the food items in the natural diet.

4. Our model provided good predictions of *in vivo* bite forces and highlighted behavioural variation that is inherent in the *in vivo* data. The temporalis generates the highest moment about the temporomandibular joint (TMJ) axis, but the moment generated by the masseter is the most important variable in explaining variation among species. The dietary classification based on the hardness of the diet was more effective than traditional dietary categories in describing biomechanical differences among groups. The temporalis generated the highest proportion of the moment about the TMJ axis in species with very hard and hard diets, the masseter was most important for species with soft diets, and the medial pterygoid was most important for species with liquid diets.

5. Our results highlight the utility of combining a modelling approach with *in vivo* data when conducting ecomorphological studies, and the importance of ecological classifications that reflect functional importance of performance traits.

Key-words: biomechanics, cranial muscles, modelling, performance, Phyllostomidae

Introduction

Studies of the relationship between morphology and performance have been a cornerstone of evolutionary biology for the last 50 years (reviewed in Garland & Losos 1994; Koehl 1996; Wainwright 1994; Irschick *et al.* 2008). Performance, the ability to carry out ecologically relevant tasks, is considered the link between morphology, ecology and fitness (Huey & Stevenson 1979; Arnold 1983; Wainwright 1994). Many biologists have studied performance traits relevant to fitness, particularly with respect to locomotion and feeding (e.g. Herrel *et al.* 2005; Calsbeek, Irschick & Pfenning 2007;

*Correspondence author. E-mail: ssantana@bio.umass.edu

Scales, King & Butler 2009; Losos 1990; Irschick 2002). In terms of feeding, bite force is a widely used performance measure that can be linked not only to morphological features of the masticatory system, but also to the mechanical demands of the species' natural diet and thus their dietary ecology (reviewed in Anderson, Mcbrayer & Herrel 2008). In fact, associations between bite force and dietary ecology have been described in sharks (Huber *et al*. 2005, Huber *et al*. 2008), lacertid lizards (Verwaijen, Van Damme & Herrel 2002; Herrel *et al*. 2001c, Herrel & Holanova 2008b), Darwin's finches (Herrel *et al*. 2005), and bats (Aguirre *et al*. 2003, Nogueira, Peracchi & Monteiro 2009), to name a few. In some of these examples, dietary hardness was either directly measured or animals were classified into categories that were considered to match the mechanical demands imposed by diet (e.g. molluscivorous lizards eat hard prey, Herrel & Holanova 2008b; Freeman 1979, 2000). Studies like these, which compare cranial form considering the material properties of foods, are likely to demonstrate stronger associations between cranial morphology and bite force than are studies that rely on more loosely-defined dietary categories such as frugivory or insectivory.

Most studies that investigate how variation in cranial morphology is related to feeding ecology through bite force are correlational. However, the underlying mechanics of bite force production have been investigated in several non-human vertebrates, including sharks (Huber *et al*. 2005), crocodiles (Cleuren, Aerts & De Vree 1995), lizards (e.g. Herrel, Aerts & De Vree 1998, 2001a), and domestic dogs (Ellis *et al*. 2009). These types of studies are more informative than correlations because they can pinpoint specific morphological features associated with variation in bite force production within and among species. Ultimately, selection on these morphological features may be a more reliable reflection of selection on whole-organism performance. Furthermore, mechanistic models of bite force production provide researchers with the tools to more accurately predict bite force when it cannot be measured directly.

The mechanistic link between variation in cranial morphology and measured bite performance has scarcely been investigated in wild mammals. Nevertheless, mammals are an ideal system for this purpose because their feeding system is relatively simple; it consists of a single bilateral articulation between the lower jaw and cranium that is, with a few exceptions, solidly fused in adults. Moreover, there is ample natural variation in cranial shape that appears to translate into variation in bite force (e.g. Aguirre *et al*. 2002; Nogueira, Peracchi & Monteiro 2009). Biomechanical models of mammal skulls predict that bite force increases as the bite point is positioned more closely to the attachment sites of the jaw adductor muscles (Spencer 1998; Greaves 2000, 2002), and mammals with short rostra produce relatively higher bite forces than mammals with longer rostra (Aguirre *et al*. 2002; Nogueira, Peracchi & Monteiro 2009; Dumont, Herrel, Medellin *et al*. 2009). The capacity to generate force is also determined by the muscles' physiological cross sectional areas (a function of muscle mass, muscle fibre length, and pennation angle), stress value(s), and relative position with respect to the temporomadibular joint (TMJ). Mammals can also modulate their bite force behaviourally, by changing the teeth used during biting, with more posterior teeth yielding higher bite forces (Dumont 1999; Dumont & Herrel 2003; Santana & Dumont 2009), and changing the activation patterns of their cranial muscles (e.g. De Gueldre & De Vree 1988; Spencer 1998; Ross *et al*. 2007; Williams *et al*. 2007; Vinyard *et al*. 2008).

Within mammals, New World leaf-nosed bats (Family Phyllostomidae) provide an excellent system for studying the relationship among cranial morphology, feeding performance, and dietary ecology because they are exceptionally diverse in these three factors (e.g. Gardner 1977; Freeman 2000; Wetterer, Rocman & Simmons 2000; Aguirre *et al*. 2002). Bite force data are relatively easy to gather from phyllostomids, and previous studies have documented correlations between their skull morphology, bite performance and diet. Bite force is highly correlated with skull size and, upon correcting for size, bite force patterns follow the predictions of the biomechanical models described above (Freeman 2000; Aguirre *et al*. 2002, 2003; Van Cakenberghe, Herrel & Aguirre 2002; Nogueira, Peracchi & Monteiro 2009). Despite many excellent descriptive studies of the cranial musculature of bats (e.g. Mcallister 1872; Storch 1968; Czarnecki & Kallen 1980), little is known about how the functional components of the masticatory apparatus vary across phyllostomids and interact to produce bite force. From a dataset spanning several bat families, Herrel *et al*. (2008a) used a static bite force model to show that variation in bite force can be predicted by differences in characteristics of the cranial muscles. Here we build on this study and investigate how the morphology of both bones and muscles interact to generate moments about the TMJ. Specifically, we explore the relationship between variation in these biomechanical parameters and differences in dietary ecology among species.

To identify important biomechanical parameters affecting bite force, we developed a 3D bite force model that integrates data describing the cranial muscles and skull morphology of 24 species of phyllostomids and one species from a closely related family (Noctilionidae). We use the bite force model to: (i) predict voluntary bite forces measured in the field, (ii) compare the variation in predicted and measured bite forces, (iii) determine the most influential biomechanical determinants of bite force in phyllostomids, and (iv) investigate how these biomechanical determinants of bite force vary among species with different diets. We hypothesize that variation in bite force in phyllostomids is closely associated with variation in the morphology of the cranial muscles and skull (as opposed to behavioural variation), and predict that interspecific differences in bite force can be explained by biomechanical variables that emerge from the bite force model. We also hypothesize that, because of differences in the physical demands among diets, bats with different diets will differ in the relative importance of the biomechanical variables responsible for generating bite force. We predict bats that specialize in diets composed by hard food items (vertebrates,

large fruit) will have a higher moment about the TMJ axis produced by the temporalis because of the need to produce high bite forces at high gape angles, whereas bats that specialize in softer food items (small fruits and insects) will have a higher moment about the TMJ axis produced by the masseter because of the need to produce high bite forces at low gape angles.

Materials and methods

BITE FORCE AND DIETARY DATA

We collected data on 24 phyllostomid and one closely related non-phyllostomid species (*Noctilio albiventris*) at localities in Venezuela (2006, 2007), Panama (2007), and Mexico (Dumont *et al.* 2009). We used mist nets to capture bats in primary and secondary succession forest sites. Following capture, we determined the bats' age class (adult vs. subadult), sex, and reproductive status. We only used adult males and adult non-pregnant, non-lactating females for this study. Shortly after capture, we measured the bats' voluntary bite force at the canines and molars using a piezoelectric force transducer (Kistler, type 9203, range ± 500 N, accuracy 0·01–0·1 N; Amherst, NY, USA) attached to a handheld charge amplifier (Kistler, type 5995, Amherst, NY, USA) (Herrel *et al.* 1999). The force transducer was mounted between two bite plates as described in Herrel *et al.* (1999). The tips of the bite plates were covered with medical tape to protect the bats' teeth and to provide a non-skid surface. We adjusted the distance between the bite plates for each individual to accommodate a gape angle of about 30° (Dumont & Herrel 2003). We recorded at least five measurements for each bat during bilateral biting at the canines and bilateral biting at the molars.

Following bite force measurements, we recorded body mass (g) using a spring scale, and head dimensions (head length, width, and height in mm) using digital callipers. Head length was measured as the distance from the tip of the rostrum to the back of the skull. Head width was measured at the broadest part of the zygomatic arches, and head height was measured at the highest part of the skull, posterior to the orbit, to the underside of the mandible. Voucher specimens of individuals with complete bite force data were retained and preserved in 70% ethanol (sample sizes in Table S1 in Supporting Information). All procedures were approved by the Institutional Animal Care and Use Committee of the University of Massachusetts, Amherst, USA (protocol # 26-10-06).

Species were classified according to diet based on two different criteria (Table S2 in Supporting Information). First, we classified species into dietary categories traditionally used to describe phyllostomid diets (i.e. insectivore, frugivore, nectarivore, sanguivore, carnivore, omnivore). Second, because bite force is associated with the mechanical challenges imposed by food items (Aguirre *et al.* 2003; Freeman & Lemen 2007), we classified species according to the theoretical hardness of their diet (i.e. liquid, soft, medium, hard, very hard). Both classifications were informed by previous dietary records (Howell & Burch 1973; Gardner 1977, Snow, Jones & Webster 1980; Ferrarezi & Gimenez 1996; Aguirre *et al.* 2003; Giannini & Kalko 2004, 2005; Da Silva, Gaona & Medellin 2008). In the case of dietary hardness, our classification was also informed by puncture resistance measurements performed on fruits and insects reported in the diet of the species (data not shown, Santana & Dumont 2009; Dechmann, Santana & Dumont 2009).

MORPHOLOGICAL DATA

Using the voucher specimens, we dissected all the major cranial muscles (musculus masseter, m. zygomaticomandibularis, m. temporalis superficialis, m. temporalis medius, m. temporalis profundus, m. pterygoideus medius, m. pterygoideus lateralis, and m. digastricus; Fig. 1a) under a binocular microscope (Zeiss Stemi SV11, Carl Zeiss, Germany). Digital pictures were taken during all stages of the dissection to document muscle insertion areas. Muscles were removed from both sides of the skull, blotted dry and weighed to the nearest 0·001 g using a high precision balance (Sauter Type 414, Sauter of America Inc., New York, NY, USA). Each muscle was transferred to a porcelain spot plate containing a 10% aqueous nitric acid solution and left until the muscle began to come apart and muscle fibres were apparent, typically after 48 h. We then slowly replaced the nitric acid solution with a 50% glycerol (v/v) aqueous solution and transferred each muscle to a microscope slide. Under the dissecting microscope, we used fine needles to separate 15–20 individual muscle fibres. We measured the length of these fibres to the nearest 0·1 mm using the microscope's ocular reticle (data in Table S1 in Supporting Information).

Physiological cross sectional areas (PCSA) were calculated for each muscle using the standard equation: PCSA = muscle mass/density × fibre length (Lieber 2002). We used a mammalian muscle density of 1·06 g cm^{-3} (Mendez & Keys 1960). The PCSA values were scaled

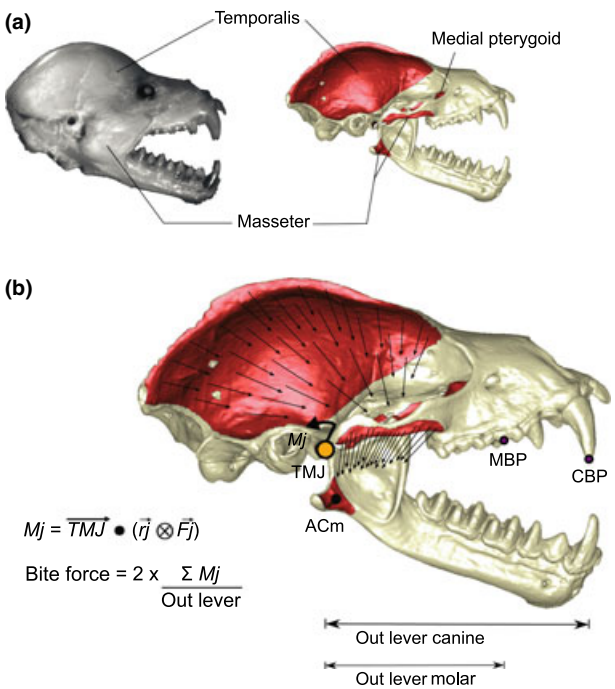

Fig. 1. (a) Photograph of the head of a phyllostomid bat (*Phyllostomus elongatus*) after removal of the skin (left) and surface model of its skull (right) showing the attachment areas of three of the most important jaw adductor muscles; (b) Surface model showing the muscle forces (black arrows) distributed across their respective attachment regions on the skull. Muscle forces are directed towards the centroid of the insertion region of each muscle on the mandible (black circle, only shown for the masseter). Muscles generate a moment (Mj) about the temporomandibular joint (TMJ). Bite forces are calculated by dividing the total moment generated by all cranial muscles by the out lever at the respective biting position (canine and molar). See text for further explanation on equations. ACm: area centroid of the masseter, CBP: canine bite point, MBP: molar bite point.

using a muscle stress of 25 N cm^{-2} (Herzog 1994) to obtain muscle force estimates. All jaw adductor muscles, with the exception of the zygomaticomandibularis, which contributed little to overall PCSA, were included in our bite force model. The PCSAs for all three parts of the temporalis were summed and this muscle was modelled as a whole (Table S2).

We cleaned the skulls of the voucher specimens using a dermestid beetle colony and scanned these skulls using a microCT-scanner (Skyscan 1172 Microfocus X-radiographic Scanner, Skyscan, Belgium) at Amherst College, Amherst MA. Details of scanning parameters are available from the authors upon request. The X-ray projection images produced by the microCT-scanner were converted into a volume consisting of a stack of X-ray attenuation cross sections, or slices, using the reconstruction software NRecon v. 1.5.1.4 (MicroPhotonics Inc., Allentown, PA, USA). The slices were imported into Mimics v. 13.0 (Materialise, Ann Arbor, MI, USA), where a thresholding tool was used to isolate the range of gray-scale values representing the skull bones. Finally, a three-dimensional volume model of each skull was produced and saved as a *.STL (surface) file.

We manipulated the surface models of the skulls using Geomagic v. 11 (Geomagic, Research Triangle Park, NC, USA) to open the jaw to a gape angle of 30 °. Assuming bilateral symmetry, we defined the areas of attachment on the right side of the skull and mandible for the m. temporalis, m. masseter, m. pterygoideus medius, and m. pterygoideus lateralis, as well as the glenoid fossae. These areas were based on the photo documentation gathered during the muscle dissections. Muscle areas were exported as surface models (NASTRAN files) to input into the bite force model software.

BITE FORCE MODEL

To mimic our *in vivo* bite force data, we used a three dimensional lever model (Davis *et al.* in press) to calculate bite forces during bilateral canine and bilateral molar biting (Fig. 1b). A Matlab program (Boneload, available from JLD upon request) was written for this purpose. The inputs for the program are: (i) the muscle attachment areas defined on the surface model of the skull (NASTRAN file), (ii) individual muscle force magnitudes, (iii) coordinates for the centroid of the muscles' insertion regions on the lower jaw, and (iv) coordinates defining the TMJ axis, which is the vector connecting the area centroid of the left and right glenoid fossae on the skull. Area centroids were calculated using the program Area_Centroids_From_STL (available from JLD upon request).

The algorithm first applies a uniform pressure on each surface triangle within the muscle attachment region on the skull. This pressure was equal to the total muscle force divided by the area of the muscle's attachment region. Next, each muscle force was directed toward the area centroid of its respective insertion region on the mandible (Fig. 1b). The resultant moment vector created by each muscle force was obtained through a vector cross product (indicated in Equation 1 by $\otimes$) between $\overrightarrow{r_j}$, the vector that defines the location of the force vector on the attachment region relative to one of the TMJs, and $\overrightarrow{F_j}$, the force vector applied to the attachment region. The resultant moment vector generates a moment (M_j) about the TMJ axis ($\overrightarrow{TMJ}$), which may be calculated using the equation:

$$M_j = \overrightarrow{TMJ} \bullet \left(\overrightarrow{r_j} \otimes \overrightarrow{F_j}\right) \quad (1)$$

where $\bullet$ denotes a vector dot product, between the vector defining the TMJ axis and the resultant moment vector.

For each individual, the moments about the TMJ axis were summed across all muscles. Bite force estimates were obtained by dividing this total moment by the out lever (perpendicular distance from the bite point to the TMJ axis) and multiplying it by two to account for bilateral biting (Fig. 1b). The out lever was measured from the surface models using Geomagic. We measured the out levers as the perpendicular distances from the tip of the canine to the TMJ axis for canine bites, and from the centre of the occlusal surface of the first molar to the TMJ axis for molar bites. Individual bite forces were predicted for each voucher specimen using the bite force model, and were averaged to obtain species means for each bite type (Table S4 in Supporting Information).

STATISTICAL ANALYSES

Means of traits for species can not be considered as statistically independent data points because of differing amounts of shared phylogenetic history (Felsenstein 1985). Therefore, we tested all variables for phylogenetic effects by calculating the parameter lambda in BayesTraits (Beta v. 1.1, Pagel & Meade 2007) using a pruned version of the Jones *et al.* (2002) and Jones, Bininda-Emonds and Gittleman (2005) species-level supertree of bats. Individual variables did not exhibit a significant phylogenetic signal (lambda = 0, $P > 0{\cdot}05$). In the context of regression, the residuals also did not have a phylogenetic signal (lambda = 0, $P > 0{\cdot}05$) and therefore we carried out the subsequent analyses without phylogenetic corrections.

To determine how well our model predicted measured bite forces, we conducted a Reduced Major Axis (RMA) regression of species means of measured bite force (response variable) against species means of predicted bite force (predictor variable). To compare the magnitude of variation in measured and predicted bite forces, we calculated coefficients of variation for each species and bite type (bilateral canine and bilateral molar) and compared them using a Wilcoxon signed-rank test. Since variation in bite force in phyllostomids is influenced by animal size (Aguirre *et al.* 2002), we also conducted this analysis on size-corrected bite forces (i.e. residual bite force from the regression using the best size predictor, see below).

We used moments produced by each muscle about the TMJ axis, which were calculated from the bite force model, as our biomechanical variables. We determined which biomechanical variables were the best predictors of bite force among species by using Akaike's Information Criterion corrected for small sample sizes (AICc, Hurvich, Simonoff & Tsai 1998). This allowed us to select the regression equation that best explained the variation in measured bite forces. The slope and intercept values for this equation were obtained through a simple regression of measured bite forces on the best biomechanical predictor.

Finally, to investigate how species with different diets differed in biomechanical variables, we classified species according to the two dietary criteria described above (items in the diet and dietary hardness, Table S2). Within each classification scheme, we conducted a discriminant analysis to separate groups of bats with different diets based on the proportion of moment about the TMJ axis generated by each muscle to the total moment about the TMJ axis during molar bites (Table S3 in Supporting Information). We used molar bites because they are universally important during feeding behaviours and represent maximum performance in the species under study: canine biting is less common (Dumont 1999; Santana & Dumont 2009). All statistical analyses were carried out in SPSS for windows (SPSS Inc., Chicago, IL, USA).

Results

MEASURED AND PREDICTED BITE FORCES

The variation in bite forces measured in the field was greater than the variation in predicted bite forces (Wilcoxon signed-rank test, canine bites: $Z = -3{\cdot}462$, $P = 0{\cdot}001$, molar bites: $Z = -3{\cdot}201$, $P = 0{\cdot}001$). The variation in the measured bite forces tended to be 2·40–2·92 times greater than the predicted bite forces, as illustrated by the error bars in Fig. 2c. We obtained a very similar result for size-corrected bite forces, indicating that the greater variation in measured bite forces is due to factors other than variation in size among the individuals sampled.

Despite variation in measured bite forces, predicted bite force was a good predictor of both measured canine and measured molar bite forces (Table S4, Fig. 2; canine bites: $r^2 = 0{\cdot}655$, $P < 0{\cdot}0001$; molar bites: $r^2 = 0{\cdot}724$, $P < 0{\cdot}0001$). The slopes of both regressions did not differ significantly from one (canine bites: $t = 6{\cdot}824$, $P < 0{\cdot}0001$, 95% confidence interval: 0·806–1·507; molar bites: $t = 7{\cdot}768$, $P < 0{\cdot}0001$, 95% confidence interval: 0·787–1·358), and the intercepts did not differ significantly from zero (canine bites: $t = 1{\cdot}135$, $P = 0{\cdot}268$, 95% confidence interval: −0·793–2·722; molar bites: $t = 1{\cdot}595$, $P = 0{\cdot}124$, 95% confidence interval: −0·501–3·881). Therefore, our bite force model reliably predicts bite force among the species studied here.

Variation in bite force among phyllostomids has been reported to be explained mostly by size (Aguirre *et al*. 2002; Nogueira, Peracchi & Monteiro 2009). However, our bite force model provided a better fit when predicting both canine bite and molar bite forces than size measurements alone. The best size predictor for canine bite force was head width ($r^2 = 0{\cdot}602$, $\beta_1 = 0{\cdot}935 \pm 0{\cdot}159$, $t = 5{\cdot}899$, $P < 0{\cdot}001$), while the best size predictor for molar bite force was head height ($r^2 = 0{\cdot}636$, $\beta_1 = 1{\cdot}476 \pm 0{\cdot}233$, $t = 6{\cdot}341$, $P < 0{\cdot}001$). Both of the models including only size measurements also included an intercept that differed significantly from zero (canine bites: $-5{\cdot}669 \pm 2{\cdot}017$, $P = 0{\cdot}01$; molar bites: $11{\cdot}691 \pm 3{\cdot}267$, $P = 0{\cdot}02$).

BIOMECHANICAL PREDICTORS OF BITE FORCE

For both canine and molar bites, the regression model that best predicts bite force includes only the moment generated about the TMJ axis by the masseter (Table 1). In turn, the moment about the TMJ axis generated by the masseter is very well predicted ($r^2 = 0{\cdot}988$, $P < 0{\cdot}001$) by the mass of this muscle ($\beta_1 = 134{\cdot}034 \pm 8{\cdot}880$, $t = 15{\cdot}094$, $P < 0{\cdot}0001$) and its fibre length ($\beta_1 = -0{\cdot}890 \pm 0{\cdot}265$, $t = -3{\cdot}363$, $P = 0{\cdot}003$). Thus, phyllostomid bats in our dataset achieve absolutely higher bite forces by having bigger masseter muscles composed of shorter masseter muscle fibres.

Species differed in the relative contribution of each muscle to the total moment about the TMJ axis depending on the dietary classification used. For traditional dietary categories, the groups only differed in the proportion of the moment about the TMJ axis generated by the masseter (Wilk's lambda = 0·588, $F_{4,20} = 3{\cdot}498$, $P = 0{\cdot}025$), and average correct classification rates were relatively low (56·0% of original groups, 32·0% of cross-validated groups). Conversely, when species were classified according to dietary hardness, three of the four muscle groups emerged as significant (temporalis: Wilk's lambda = 0·486, $F_{4,20} = 5{\cdot}297$, $P = 0{\cdot}004$;

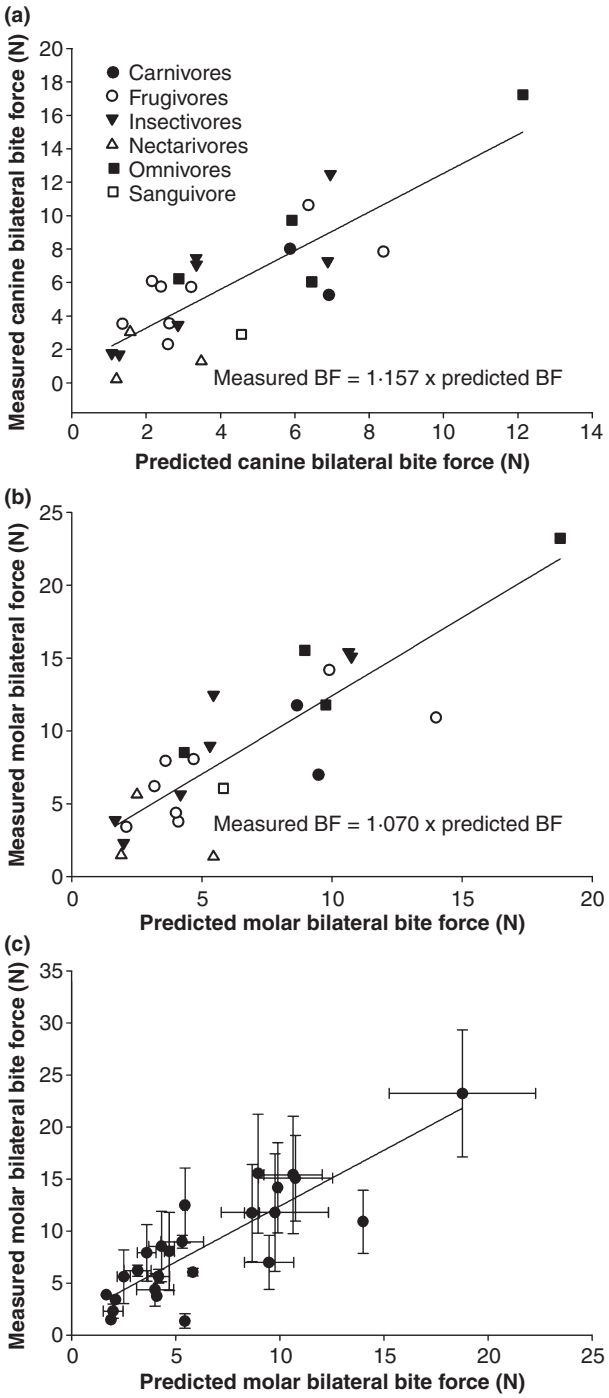

Fig. 2. Bite forces (BF) predicted using our 3D method versus *in vivo* measured bite forces for the species included in this study: (a) canine bilateral bites, (b) molar bilateral bites, and (c) molar bilateral bites presenting standard deviation bars. See text for detailed regression statistics.

Table 1. Parameters for the regression models of measured canine and molar bite forces on the moment about TMJ by the m. masseter

	Estimate ± SE	95% CI	*t*	*P*	r^2	AICc
Canine bites						
Slope	0·792 ± 0·104	0·577–1·007	7·624	0·000	0·717	39·272
Intercept	2·702 ± 0·591	1·480–3·924	4·575	0·000		
Molar bites						
Slope	1·164 ± 0·118	0·919–1·409	9·827	0·000	0·808	45·839
Intercept	3·956 ± 0·673	2·562–5·349	5·873	0·000		

masseter: Wilk's lambda = 0·367, $F_{4,20}$ = 8·637, $P < 0·0001$; medial pterygoid: Wilk's lambda = 0·473, $F_{4,20}$ = 5·564, P = 0·004), and average correct classification rates were relatively high (76% of original groups, 60% of cross-validated groups). Among these groups the temporalis generated the highest proportion of the moment about the TMJ axis in species with very hard and hard diets (0·835 ± 0·046%), whereas the masseter was most important for species with soft diets (0·169 ± 0·011%), and the medial pterygoid was most important for species with liquid diets (0·141 ± 0·059%). Other categories (medium and hard diets) presented intermediate values.

Discussion

Ecomorphological studies have demonstrated mechanistic links between cranial morphology, bite force and feeding ecology for only a handful of vertebrate species (e.g. Cleuren, Aerts & De Vree 1995; Herrel, Aerts & De Vree 1998; Herrel *et al*. 2001c; Huber *et al*. 2005). The main obstacle to establishing these connections lay in building models that accurately represent the mechanics of the feeding apparatus by incorporating data summarizing both muscle anatomy and lever mechanics, and gathering bite force data from wild animals to validate these models. Here we present a comprehensive dataset on bite force and cranial geometry that has allowed us to model the mechanism of bite force production in a morphologically diverse clade of mammals, and to investigate how species may be functionally specialized for different diets.

Even though our model predicted bite forces with relatively high accuracy, it is important to note that it does not incorporate behavioural variation. This is illustrated by a greater intraspecific variation in *in vivo* bite forces than in predicted bite forces. It is not uncommon for *in vivo* performance measurements to vary greatly due to differences in motivation among individuals. In fact, studies of bite forces in vertebrates report standard deviations as high as 56% of the mean bite forces (e.g. Herrel *et al*. 1999, 2005; Herrel, De Grauw & Lemos-Espinal 2001b). Likely sources of variation probably include differential activation patterns of the jaw-closing muscles and individual animal's motivation to bite. Another interesting, albeit untested, possibility is the temporal or geographic variation in intraspecific bite force in response to variation in food resources or hormonal state (Irschick *et al*. 2006). Since the samples for many species included here are composed of individuals from different localities, our data could be susceptible to this potential source of variation. A more detailed study is necessary to test this idea. Whatever the cause, this study highlights the value of not only validating biomechanical models using *in vivo* bite performance data, but measuring bite force in multiple individuals to document variation.

Despite individual variation, our 3D model predicted measured bite forces more accurately than size alone. In addition to size, previous studies have demonstrated that skull shape is also important in determining interspecific differences in bite force. Specifically, Nogueira, Peracchi & Monteiro (2009) found that, in phyllostomids, size-corrected bite forces were correlated with shorter rostra, alignment of the molars along the masseter insertion region, and expansion of the anterior zygomatic arch and angular process, both of which are sites of insertion of the masseter. Based on these findings, Nogueira *et al*. hypothesized that the masseter is of great importance in bite force production. Even though our results indicate that the temporalis generates the greatest moment about the TMJ, our data supports Noguiera's hypothesis, as the moment generated by masseter is the variable that best explains variation in measured bite force. In contrast, our study did not replicate work by Herrel *et al*. (2008a), who found that variation in measured bite force in a sample of bats species (including non-phyllostomids) was best explained by residual temporalis mass and skull length. In addition to being limited to phyllstomids, our study built on Herrel *et al*.'s work to explore how muscle forces and attachment regions work together to produce different moments about the TMJ. The different conclusions reached by these two studies likely can be attributed to some combination of their different approaches to understanding bite force and choice of taxa.

The fact that variation in bite force among phyllostomids is best explained by the masseter could be related to the species' feeding behaviour and ecology. For mammals in general, variation in cranial and muscle morphology is associated with variation in loading regimes and the ability to generate bite forces at different gape angles. Specifically, different morphologies confer differences among muscles in their lever mechanical advantage and ability to produce moments about the TMJ axis (Dumont, Piccirillo & Grosse 2005; Turnbull 1970; Slater & Van Valkenburgh 2009; Dumont *et al*. in press). Mammals that require high bite forces at high gape angles tend to have the largest moment about the TMJ axis produced by the temporalis (e.g. carnivores, Greaves 1985; Slater, Dumont & Van Valkenburgh 2009; but see Williams, Peiffer & Ford 2009), whereas mammals that require high bite forces at low gapes tend to have the largest moment about the TMJ axis produced by the masseter (e.g. herbivores, Herring & Herring 1974; Greaves 2000). Most of the species included here rely on the use of their molar teeth to crush insects or to bite and macerate fruit pulp, which require low gape angles during most phases of fruit processing (Dumont 1999;

Dumont *et al.* 2009; Santana & Dumont 2009). Since more than half of the species in our sample utilize plant resources, particularly fruits, it is possible that pulp chewing is an important activity that may have fitness consequences.

With respect to feeding ecology, we found that a dietary classification that reflects the mechanical demands of a species' food items is superior to traditional dietary categories in establishing differences in biomechanical specializations among species. The fact traditional dietary categories do not necessarily reflect functional categories suggests that other conventional 'functional' groupings, such as those based on echolocation call structure and diet, may be improved by more detailed investigations of the underlying mechanics. A functional approach has been previously used to characterize the ecology of several vertebrate species and investigate the link between ecology and morphology (Freeman 1979; Losos 1992; Herrel, O'reilly & Richmond 2002; Huber *et al.* 2005). Functional approaches of this kind have not been explicitly used to investigate measured bite force and dietary ecology in bats. As a potential consequence, previous studies have faced difficulties in identifying morphological or performance differences among dietary categories (Nogueira, Peracchi & Monteiro 2009; Aguirre *et al.* 2002; but see Freeman 1979; Van Cakenberghe, Herrel & Aguirre 2002). Nectarivorous and sanguivorous bats are a notable exception (Freeman 1979, 1988; Nogueira, Peracchi & Monteiro 2009), probably because these bats feed on food resources that clearly have different mechanical demands than fruits, insects and vertebrates. In contrast, even though fruits and insects may differ in some mechanical properties, they may not necessarily differ in hardness, the aspect of diet that is immediately most relevant to bite force. Since a fruit and an insect of similar size could require the same force to process, we did not expect differences in bite force among many of the bats that were categorized as frugivores and insectivores.

There is great need for more quantitative data on the hardness of food items consumed by all animals, but we were able to identify functional dietary groups of phyllostomid bats that at least grossly match biomechanical differences of their feeding apparatus. Accordingly, bats we classified as highly durophagous (carnivores and hard-fruit specialists) are characterized by relatively high temporalis PCSA and moments, traits that are typical of other mammals specializing in hard prey (Smith & Savage 1959; Davis 1964; Perez-Barberia & Gordon 1999). The skulls of these hard-object specialists are characterized by features that allow for greater size and higher mechanical advantage of the temporalis, such as a higher coronoid process, greater development of the cranial crests, and posterior projection of the interparietal region (Freeman 1979, 1988; Nogueira, Peracchi & Monteiro 2009). At the other end of the spectrum, liquid feeders are characterized by a relatively high medial pterygoid PCSA and moments. In these bats, an elongated rostrum appears to have evolved to support the long tongue used to obtain nectar. This seems to have resulted in a trade-off with the generation of bite force by the main jaw adductors (temporalis and masseter), and has potentially resulted in a higher emphasis of the pterygoids in generating bite force.

Our study illustrates the importance of using a modelling approach that is validated with *in vivo* data when studying the mechanics behind performance traits. This approach allowed us to identify morphological and biomechanical predictors of bite performance among mammals with a wide range of cranial morphologies, and to address the relationship between these predictors and feeding ecology. Furthermore, our study emphasizes that using functional ecological classifications that are relevant to the performance traits under study can illuminate the relationships among morphology, performance and ecology more clearly than classifications that ignore function.

Acknowledgements

This research was supported by NSF IOB 07616 and NSF DBI 0743460 to ERD, a UMass Natural History Collections David J. Klingener Endowment Scholarship and a Smithsonian Tropical Research Institute Predoctoral Fellowship to SES. We thank Whitey Hagadorn for training and access to the micro-CT scanner, John W. Hermanson for advice on the protocol for muscle fibre separation, Elsbeth Walker for access to the analytical balance, Dan Pulanski for technical support, and Joseph Smith, Jaime Tanner and Tom Eiting for fruitful discussions on the manuscript.

References

Aguirre, L.F., Herrel, A., Van Damme, R. & Matthysen, E. (2002) Ecomorphological analysis of trophic niche partitioning in a tropical savannah bat community. *Proceedings of the Royal Society of London Series B-Biological Sciences*, **269**, 1271–1278.

Aguirre, L.F., Herrel, A., Van Damme, R. & Matthysen, E. (2003) The implications of food hardness for diet in bats. *Functional Ecology*, **17**, 201–212.

Anderson, R.A., Mcbrayer, L.D. & Herrel, A. (2008) Bite force in vertebrates: opportunities and caveats for use of a nonpareil whole-animal performance measure. *Biological Journal of the Linnean Society*, **93**, 709–720.

Arnold, S.J. (1983) Morphology, performance and fitness. *American Zoologist*, **23**, 347–361.

Calsbeek, R., Irschick, D.J. & Pfenning, D. (2007) The quick and the dead: correlational selection on morphology, performance, and habitat use in island lizards. *Evolution*, **61**, 2493–2503.

Cleuren, J., Aerts, P. & De Vree, F. (1995) Bite and joint force analysis in *Caiman crocodilus*. *Belgian Journal of Zoology*, **125**, 79–94.

Czarnecki, R.T. & Kallen, F.C. (1980) Craniofacial, occlusal, and masticatory anatomy in bats. *The Anatomical Record*, **198**, 87–105.

Da Silva, A.G., Gaona, O. & Medellin, R.A. (2008) Diet and trophic structure in a community of fruit-eating bats in Lacandon Forest, Mexico. *Journal of Mammalogy*, **89**, 43–49.

Davis, D.D. (1964) The giant panda: a morphological study of evolutionary mechanisms. *Fieldiana Zoology Memoirs*, **3**, 1–339.

Davis, J.L., Santana, S.E., Dumont, E.R. & Grosse, I. (in press) Predicting Bite Force in Mammals: 2D vs. 3D lever models. *Journal of Experimental Biology*.

De Gueldre, G. & De Vree, F. (1988) Quantitative electromyography of the masticatory muscles of *Pteropus giganteus* (Megachiroptera). *Journal of Morphology*, **196**, 73–106.

Dechmann, D., Santana, S.E. & Dumont, E.R. (2009) Roost making in bats - Adaptations for excavating active termite nests. *Journal of Mammalogy*, **90**, 1461–1468.

Dumont, E.R. (1999) The effect of food hardness on feeding behaviour in frugivorous bats (Phyllostomidae): an experimental study. *Journal of Zoology*, **248**, 219–229.

Dumont, E.R. & Herrel, A. (2003) The effects of gape angle and bite point on bite force in bats. *Journal of Experimental Biology*, **206**, 2117–2123.

Dumont, E.R., Piccirillo, J. & Grosse, L.R. (2005) Finite-element analysis of biting behavior and bone stress in the facial skeletons of bats. *Anatomical*

Record Part A-Discoveries in Molecular Cellular and Evolutionary Biology, **283A**, 319–330.

Dumont, E.R., Herrel, A., Medellin, R.A., Vargas, J. & Santana, S.E. (2009) Built to bite: cranial design and function in the wrinkle faced bat (*Centurio senex*). *Journal of Zoology*, **279**, 329–337.

Dumont, E.R., Davis, J.L., Grosse, I.R. & Burrows, A.M. (in press) Finite element analysis of performance in the skulls of marmosets and tamarins. *Journal of Anatomy*.

Ellis, J.L., Thomason, J., Kebreab, E., Zubair, K. & France, J. (2009) Cranial dimensions and forces of biting in the domestic dog. *Journal of Anatomy*, **214**, 362–373.

Felsenstein, J. (1985) Phylogenies and the comparative method. *American Naturalist*, **125**, 1–15.

Ferrarezi, H. & Gimenez, E.A. (1996) Systematic patterns and the evolution of feeding habits in Chiroptera (Mammalia: Archonta). *Journal of Comparative Biology*, **1**, 75–95.

Freeman, P.W. (1979) Specialized insectivoy: beetle-eating and moth-eating molossid bats. *Journal of Mammalogy*, **60**, 467–479.

Freeman, P.W. (1988) Frugivorous and animalivorous bats (Microchiroptera): dental and cranial adaptations. *Biological Journal of the Linnean Society*, **33**, 249–272.

Freeman, P.W. (2000) Macroevolution in Microchiroptera: recoupling morphology and ecology with phylogeny. *Evolutionary Ecology Research*, **2**, 317–335.

Freeman, P.W. & Lemen, C.A. (2007) Using scissors to quantify hardness of insects: do bats select for size or hardness? *Journal of Zoology*, **271**, 469–476.

Gardner, A. (1977) Feeding habits. *Biology of Bats of the New World Family Phyllostomatidae. Part II* (eds R.J. Baker, J.K.J. Jones & D.C. Carter). pp. 293–350, Special Publication of the Museum Texas Tech University, Lubbock, Texas.

Garland, T. & Losos, J.B. (1994) Ecological morphology of locomotor performance in squamate reptiles. *Ecological Morphology: Integrative Organismal Biology* (eds P.C. Wainwright & S.M. Reilly). pp. 240–302, University of Chicago Press, Chicago.

Giannini, N.P. & Kalko, E.K.V. (2004) Trophic structure in a large assemblage of phyllostomid bats in Panama. *Oikos*, **105**, 209–220.

Giannini, N.P. & Kalko, E.K.V. (2005) The guild structure of animalivorous leaf-nosed bats of Barro Colorado Island, Panama, revisited. *Acta Chiropterologica*, **7**, 131–146.

Greaves, W.S. (1985) The generalized carnivore jaw. *Zoological Journal of the Linnean Society*, **85**, 267–274.

Greaves, W.S. (2000) Location of the vector of jaw muscle force in mammals. *Journal of Morphology*, **243**, 293–299.

Greaves, W.S. (2002) Modeling the distance between the molar tooth rows in mammals. *Canadian Journal of Zoology*, **80**, 388–393.

Herrel, A., Aerts, P. & De Vree, F. (1998) Ecomorphology of the lizard feeding apparatus: a modelling approach. *Netherlands Journal of Zoology*, **48**, 1–25.

Herrel, A., Aerts, P. & De Vree, D. (2001a) Static biting in lizards: functional morphology of the temporal ligaments. *Journal of Zoology*, **244**, 135–143.

Herrel, A., De Grauw, E. & Lemos-Espinal, J.A. (2001b) Head shape and bite performance in xenosaurid lizards. *Journal of Experimental Zoology*, **290**, 101–107.

Herrel, A. & Holanova, V. (2008b) Cranial morphology and bite force in *Chamaeleolis* lizards–Adaptations to molluscivory? *Zoology*, **111**, 467–475.

Herrel, A., O'reilly, J.C. & Richmond, A.M. (2002) Evolution of bite performance in turtles. *Journal of Evolutionary Biology*, **15**, 1083–1094.

Herrel, A., Spithoven, L., Van Damme, R. & De Vree, F. (1999) Sexual dimorphism of head size in *Gallotia galloti*: testing the niche divergence hypothesis by functional analyses. *Functional Ecology*, **13**, 289–297.

Herrel, A., Van Damme, R., Vanhooydonck, B. & De Vree, F. (2001c) The implications of bite performance for diet in two species of lacertid lizards. *Canadian Journal of Zoology*, **79**, 662–670.

Herrel, A., Podos, J., Huber, S.K. & Hendry, A.P. (2005) Bite performance and morphology in a population of Darwin's finches: implications for the evolution of beak shape. *Functional Ecology*, **19**, 43–48.

Herrel, A., De Smet, A., Aguirre, L.F. & Aerts, P. (2008a) Morphological and mechanical determinants of bite force in bats: do muscles matter? *Journal of Experimental Biology*, **211**, 86.

Herring, S.W. & Herring, S.E. (1974) The superficial masseter and gape in mammals. *The American Naturalist*, **108**, 561–576.

Herzog, W. (1994) Muscle. *Biomechanics of the Musculoskeletal System* (eds B.M. Nigg & W. Herzog). pp. 154–187, John Wiley & Sons, Chichester.

Howell, D.J. & Burch, D. (1973) Food habits of some Costa Rican bats. Hábitos alimentarios de algunos murciélagos costarricenses. *Revista de Biología Tropical*, **21**, 281–294.

Huber, D.R., Eason, T.G., Hueter, R.E. & Motta, P.J. (2005) Analysis of the bite force and mechanical design of the feeding mechanism of the durophagous horn shark *Heterodontus francisci*. *Journal of Experimental Biology*, **208**, 3553–3571.

Huber, D.R., Claes, J.M., Mallefet, J. & Herrel, A. (2008) Is extreme bite performance associated with extreme morphologies in sharks? *Physiological and Biochemical Zoology*, **82**, 20–28.

Huey, R.B. & Stevenson, R.D. (1979) Integrating thermal physiology and ecology of ectotherms: a discussion of approaches. *Integrative and Comparative Biology*, **19**, 357–366.

Hurvich, C.M., Simonoff, J.S. & Tsai, C.L. (1998) Smoothing parameter selection in nonparametric regression using an improved Akaike information criterion. *Journal of the Royal Statistical Society. Series B (Statistical Methodology)*, **60**, 271–293.

Irschick, D.J. (2002) Evolutionary approaches for studying functional morphology: examples from studies of performance capacity. *Integrative and Comparative Biology*, **42**, 278–290.

Irschick, D.J., Ramos, M., Buckley, C., Elstrott, J., Carlisle, E., Lailvaux, S.P., Bloch, N., Herrel, A. & Vanhooydonck, B. (2006) Are morphology-performance relationships invariant across different seasons? A test with the green anole lizard (*Anolis carolinensis*). *Oikos*, **114**, 49–59.

Irschick, D.J., Meyers, J.J., Husak, J.F. & Le Galliard, J. (2008) How does selection operate on whole-organism functional performance capacities? A review and synthesis. *Evolutionary Ecology Research*, **10**, 177–196.

Jones, K.E., Bininda-Emonds, O.R.P. & Gittleman, J.L. (2005) Bats, clocks, and rocks: diversification in patterns in Chiroptera. *Evolution*, **59**, 2243–2255.

Jones, K.E., Purvis, A., Maclarnon, A.N.N., Bininda-Emonds, O.R.P. & Simmons, N.B. (2002) A phylogenetic supertree of the bats (Mammalia: Chiroptera). *Biological Reviews*, **77**, 223–259.

Koehl, M.A.R. (1996) When does morphology matter? *Annual Review of Ecology, Evolution, and Systematics*, **27**, 501–542.

Lieber, R.L. (2002) *Skeletal Muscle Structure, Function & Plasticity: The Physiological Basis of Rehabilitation*. Lippincott, Williams & Wilkins, Baltimore.

Losos, J.B. (1990) Ecomorphology, performance capability, and scaling of West Indian *Anolis* lizards: an evolutionary analysis. *Ecological Monographs*, **60**, 369–388.

Losos, J.B. (1992) The evolution of convergent structure in Caribbean *Anolis* communities. *Systematic Biology*, **41**, 403.

McAllister, A. (1872) The myology of the Chiroptera. *Philosophical Transactions of the Royal Society London*, **162**, 125–171.

Mendez, J. & Keys, A. (1960) Density and composition of mammalian muscle. *Metabolism*, **9**, 184–188.

Nogueira, M.R., Peracchi, A.L. & Monteiro, L.R. (2009) Morphological correlates of bite force and diet in the skull and mandible of phyllostomid bats. *Functional Ecology*, **23**, 715–723.

Pagel, M. & Meade, A. (2007) BayesTraits, version 1. 1 - Draft Manual. Website http://www.evolution.rdg.ac.uk.

Perez-Barberia, F.J. & Gordon, I.J. (1999) The functional relationship between feeding type and jaw and cranial morphology in ungulates. *Oecologia*, **118**, 157–165.

Ross, C.F., Dharia, R., Herring, S.W., Hylander, W.L., Liu, Z.J., Rafferty, K.L., Ravosa, M.J. & Williams, S.H. (2007) Modulation of mandibular loading and bite force in mammals during mastication. *Journal of Experimental Biology*, **210**, 1046.

Santana, S.E. & Dumont, E.R. (2009) Connecting behaviour and performance: the evolution of biting behaviour and bite performance in bats. *Journal of Evolutionary Biology*, **22**, 2131–2145.

Scales, J.A., King, A.A. & Butler, M.A. (2009) Running for your life or running for your dinner: what drives fiber-type evolution in lizard locomotor muscles? *The American Naturalist*, **173**, 543–553.

Slater, G.J., Dumont, E.R. & Van Valkenburgh, B. (2009) Implications of predatory specialization for cranial form and function in canids. *Journal of Zoology*, **278**, 181–188.

Slater, G.J. & Van Valkenburgh, B. (2009) Allometry and performance: the evolution of skull form and function in felids. *Journal of Evolutionary Biology*, **22**, 2278–2287.

Smith, J.M. & Savage, R.J.G. (1959) The mechanics of mammalian jaws. *School Science Review*, **40**, 289–301.

Snow, J.L., Jones Jr, J.K. & Webster, W.D. (1980) *Centurio senex*. *Mammalian Species*, **138**, 1–3.

Spencer, M.A. (1998) Force production in the primate masticatory system: electromyographic tests of biomechanical hypotheses. *Journal of Human Evolution*, **34**, 25–54.

Storch, G. (1968) Funktionsmorphologische Untersuchungen an der Kaumuskulatur und an korrelierten Schadelstrukturen der Chiropteren. *Senckenbergische Naturforschende Gesellschaft*, **517**, 1–92.

Turnbull, W.D. (1970) Mammalian masticatory apparatus. *Fieldiana Geology*, **18**, 149–356.

Van Cakenberghe, V., Herrel, A. & Aguirre, L.F. (2002) Evolutionary relationships between cranial shape and diet in bats (Mammalia: Chiroptera). *Topics in Functional and Ecological Vertebrate Morphology* (eds P. Aerts, K. D'Août, A. Herrel & R. Van Damme). pp. 205–236, Shaker Publishing, Maastricht, The Netherlands.

Verwaijen, D., Van Damme, R. & Herrel, A. (2002) Relationships between head size, bite force, prey handling efficiency and diet in two sympatric lacertid lizards. *Functional Ecology*, **16**, 842–850.

Vinyard, C.J., Wall, C.E., Williams, S.H. & Hylander, W.L. (2008) Patterns of variation across primates in jaw-muscle electromyography during mastication. *Integrative and Comparative Biology*, **48**, 294.

Wainwright, P.C. (1994) Functional morphology as a tool in ecological research. *Ecological Morphology* (eds P.C. Wainwright & S.M. Reilly). pp. 42–59, The University of Chicago Press, Chicago.

Wetterer, A.L., Rocman, M.V. & Simmons, N.B. (2000) Phylogeny of phyllostomid bats (Mammalia: Chiroptera): data from diverse morphological systems, sex chromosomes and restriction sites. *Bulletin of the American Museum of Natural History*, **248**, 1–200.

Williams, S.H., Peiffer, E. & Ford, S. (2009) Gape and bite force in the rodents *Onychomys leucogaster* and *Peromyscus maniculatus*: Does jaw-muscle anatomy predict performance? *Journal of Morphology*, **270**, 1338–1347.

Williams, S.H., Vinyard, C.J., Wall, C.E. & Hylander, W.L. (2007) Masticatory motor patterns in ungulates: a quantitative assessment of jaw-muscle coordination in goats, alpacas and horses. *Journal of Experimental Zoology Part A Comparative Experimental Biology*, **307**, 226–240.

Received 29 November 2009; accepted 22 February 2010
Handling Editor: Peter Wainwright

Supporting information

Additional Supporting Information may be found in the online version of this article.

Table S1. Muscle masses and fibre lengths.

Table S2. Dietary categories and PCSAs.

Table S3. Moments generated by each muscle.

Table S4. Predicted and measured bite forces.

As a service to our authors and readers, this journal provides supporting information supplied by the authors. Such materials may be re-organized for online delivery, but are not copy-edited or typeset. Technical support issues arising from supporting information (other than missing files) should be addressed to the authors.

Table S1: Sample sizes, mass (mg) and fiber lengths (mm) for each of the main cranial muscles in the 25 species included in this study. Data are means ± standard deviations. Zygom: m. zygomaticomandibularis, FL: fiber length.

Species	n	Temporalis		Masseter		Medial Pterygoid		Lateral Pterygoid		Zygom.		Digastric	
		mass	FL	mass	FL	mass	FL	mass	FL	mass	FL	mass	FL
Anoura geoffroyi	1	67.15	3.93	9.00	3.54	6.95	1.83	1.45	1.71	3.45	2.03	9.20	3.90
Artibeus jamaicensis	2	404.28 ± 38.86	6.17 ± 0.47	41.85 ± 6.36	3.54 ± 0.99	23.63 ± 3.22	2.93 ± 0.05	5.73 ± 2.44	2.42 ± 0.49	34.68 ± 2.58	2.99 ± 0.25	34.88 ± 4.35	5.35 ± 0.78
Carollia brevicauda	4	184.05 ± 47.60	5.17 ± 0.53	31.00 ± 7.58	4.23 ± 0.61	12.74 ± 0.67	2.65 ± 0.27	3.33 ± 0.72	2.11 ± 0.49	6.75 ± 1.41	3.07 ± 1.25	14.50 ± 2.34	4.20 ± 0.77
Carollia perspicillata	2	134.98 ± 15.66	5.26 ± 0.24	25.58 ± 4.14	3.61 ± 0.33	11.25 ± 2.05	2.42 ± 0.01	4.65 ± 1.20	2.57 ± 0.59	2.80 ± 1.13	2.24 ± 0.62	12.73 ± 0.46	4.47 ± 0.92
Centurio senex	1	137.45	3.04	3.80	1.87	7.10	1.91	3.15	1.52	8.60	1.76	11.40	5.19
Desmodus rotundus	1	270.50	4.83	32.90	4.17	21.10	2.47	3.95	2.15	15.10	1.73	24.90	9.68
Enchistenes hartii	2	105.30 ± 13.36	4.66 ± 0.57	10.95 ± 0.71	2.91 ± 0.18	8.60 ± 1.70	2.27 ± 0.22	2.83 ± 1.45	1.81 ± 0.43	7.68 ± 0.39	2.56 ± 0.60	7.95 ± 0.71	4.04 ± 0.13
Glossophaga soricina	1	254.45	4.23	11.10	2.84	4.95	1.48	1.00	1.36	2.80	1.63	8.20	4.07
Lonchophylla robusta	2	140.70 ± 8.20	4.79 ± 0.21	20.63 ± 0.74	3.98 ± 0.01	7.68 ± 1.17	1.91 ± 0.21	2.88 ± 0.39	1.68 ± 0.24	4.38 ± 0.53	1.94 ± 0.33	21.48 ± 3.15	5.25 ± 0.43
Lophostoma brasiliense	3	159.60 ± 20.69	3.68 ± 0.54	16.67 ± 2.99	2.68 ± 0.73	7.35 ± 0.87	2.25 ± 0.46	1.62 ± 0.58	1.63 ± 0.33	8.22 ± 0.45	1.90 ± 0.25	12.40 ± 2.28	3.82 ± 0.44
Lophostoma silvicolum	2	461.18 ± 87.50	4.59 ± 0.46	49.70 ± 4.74	4.11 ± 0.37	18.65 ± 3.18	2.72 ± 0.13	7.10 ± 0.78	2.66 ± 0.17	26.20 ± 3.46	2.29 ± 0.09	45.95 ± 5.44	4.89 ± 1.54
Micronycteris hirsuta	3	207.27 ±6.08	4.50 ± 0.22	28.95 ± 4.55	3.43 ± 0.15	10.13 ± 0.67	2.70 ± 0.36	2.72 ± 0.85	1.63 ± 0.05	18.28 ± 2.33	2.40 ± 0.12	19.30 ± 0.43	4.56 ± 0.71

Table S1 (continued).

Species	n	Temporalis		Masseter		Medial Pterygoid		Lateral Pterygoid		Zygom.		Digastric	
		mass	FL	mass	FL	mass	FL	mass	FL	mass	FL	mass	FL
Micronycteris megalotis	2	53.03 ± 8.38	3.29 ± 0.31	7.83 ± 0.88	2.29 ± 0.06	3.50 ± 0.71	1.52 ± 0.30	0.80 ± 0.71	1.51 ± 0.23	5.43 ± 0.88	2.29 ± 0.54	5.13 ± 1.17	3.26 ± 0.66
Micronycteris minuta	1	52.20	3.44	7.45	± 2.65	4.35	2.07	0.95	1.33	6.60	2.22	5.75	3.80
Mimon crenulatum	4	174.48 ± 27.24	3.82 ± 0.73	19.90 ± 3.38	2.97 ± 0.51	9.18 ± 1.72	2.23 ± 0.03	3.05 ± 1.23	1.59 ± 0.59	18.10 ± 0.35	3.16 ± 1.23	14.98 ± 1.28	3.80 ± 1.10
Noctilio albiventris	2	390.93 ± 25.84	4.70 ± 0.57	20.45 ± 1.41	3.49 ± 0.76	17.48 ± 4.63	3.27 ± 0.72	7.60 2.12	1.95 ± 0.01	16.65 ± 2.26	2.75 ± 0.14	30.65 ± 3.68	4.48 ± 1.05
Phylloderma stenops	2	411.63 ± 2.30	6.21 ± 0.43	71.93 ± 4.42	5.07 ± 0.18	30.00 ± 0.00	3.68 ± 0.32	12.05 ± 4.17	2.19 ± 0.26	36.05 ± 1.41	3.67 ± 0.95	40.48 ± 2.72	8.10 ± 4.31
Phyllostomus elongatus	2	439.58 ± 76.76	5.03 ± 0.59	67.98 ± 5.69	4.26 ± 0.03	24.15 ± 0.21	2.86 ± 0.22	5.33 ± 0.53	2.49 ± 0.25	48.85 ± 1.98	3.48 ± 0.47	47.60 ± 7.71	7.66 ± 1.96
Phyllostomus hastatus	2	1146.58 ± 277.50	6.41 ± 0.38	155.78 ± 47.27	6.08 ± 0.18	47.75 ± 15.20	4.13 ± 0.75	17.93 ± 11.49	2.49 ± 0.24	94.80 ± 26.45	4.01 ± 0.47	131.15 ± 30.19	10.37 ± 0.37
Sphaeronycteris toxophyllum	1	98.25	3.69	4.20	± 2.16	5.45	1.78	2.00	2.15	5.75	2.64	8.60	4.46
Sturnira lilium	2	186.60 ± 42.57	5.39 ± 0.58	25.35 ± 4.60	4.42 0.76	14.80 ± 0.07	2.46 ± 0.23	4.85 ± 0.28	2.50 ± 0.62	10.50 ± 2.40	3.08 ± 0.11	16.73 ± 2.23	5.77 ± 0.33
Tonatia saurophila	3	406.63 ± 25.19	4.96 ± 0.48	51.10 ± 2.84	3.93 ± 0.58	16.82 ± 5.89	2.70 ± 0.61	4.38 ± 1.16	1.48 ± 0.26	32.55 ± 1.43	2.82 ± 0.45	33.70 ± 1.53	4.52 ± 0.49
Trachops cirrhosus	4	362.90 ± 73.52	4.84 ± 1.16	40.49 ± 12.75	4.58 ± 0.67	19.43 ± 1.82	2.81 ± 0.75	9.34 ± 2.25	2.29 ± 1.00	20.18 ± 5.86	2.53 ± 0.85	36.69 ± 6.42	5.65 ± 0.42
Uroderma bilobatum	2	140.05 ± 6.29	4.89 ± 0.66	15.53 ± 2.86	3.16 ± 0.98	10.38 ± 1.73	2.18 ± 0.50	2.30 ± 1.34	1.26 ± 0.40	14.03 ± 0.88	2.01 ± 0.19	11.98 ± 0.60	4.98 ± 1.22
Vampyressa pusilla	1	46.95	3.47	4.15	3.64	6.15	1.40	1.30	1.26	6.05	2.57	5.00	4.00

Table S2: Sample sizes, dietary categories and mean (± standard deviation) physiological cross sectional areas (PCSA, in mm^2) for the 25 species included in this study. PCSAs for the m. temporalis are the summation the PCSAs of its three parts (superficialis, medius, profundus).

Species	N	Diet	Dietary hardness	PCSA (mm^2)			
				Temporalis	Masseter	Medial Pterygoid	Lateral Pterygoid
Anoura geoffroyi	1	Nectarivore	Liquid	15.77	2.4	3.58	0.8
Artibeus jamaicensis	2	Frugivore	Hard	57.62 ± 0.8	11.85 ± 5.01	7.61 ± 0.91	2.38 ± 1.43
Carollia brevicauda	4	Frugivore	Soft	31.43 ± 5.96	7.03 ± 1.91	4.59 ± 0.75	1.55 ± 0.48
Carollia perspicillata	2	Frugivore	Soft	23.8 ± 0.93	6.66 ± 0.48	4.4 ± 0.81	1.7 ± 0.05
Centurio senex	1	Frugivore	Very Hard	38.14	1.92	3.51	1.96
Desmodus rotundus	1	Sanguivore	Liquid	51.5	7.44	8.05	1.73
Enchistenes hartii	2	Frugivore	Hard	20.96 ± 5.49	3.56 ± 0.01	3.63 ± 1.06	1.61 ± 1.14
Glossophaga soricina	1	Nectarivore	Liquid	56.54	3.69	3.16	0.69
Lonchophylla robusta	2	Nectarivore	Liquid	26.91 ± 1.15	4.89 ± 0.16	3.85 ± 1	1.62 ± 0.01
Lophostoma brasiliense	3	Insectivore	Medium	39.21 ± 6.23	6.01 ± 1.02	3.17 ± 0.71	0.98 ± 0.43
Lophostoma silvicolum	2	Insectivore	Medium	87.66 ± 28.06	11.52 ± 2.14	6.5 ± 1.41	2.53 ± 0.43
Micronycteris hirsuta	3	Insectivore	Medium	39.72 ± 1.67	8 ± 1.6	3.58 ± 0.55	1.58 ± 0.53
Micronycteris megalotis	2	Insectivore	Medium	15.74 ± 3.58	3.23 ± 0.44	2.26 ± 0.88	0.54 ± 0.53
Micronycteris minuta	1	Insectivore	Medium	14.42	2.65	1.99	0.68
Mimon crenulatum	3	Insectivore	Medium	41.76 ± 1.52	6.44 ± 1.68	3.89 ± 0.72	1.87 ± 0.81
Noctilio albiventris	2	Carnivore	Very Hard	73.77 ± 1.74	5.62 ± 0.85	5.02 ± 0.23	3.67 ± 1
Phylloderma stenops	2	Omnivore	Medium	61.09 ± 2.63	13.42 ± 1.29	7.73 ± 0.67	5.35 ± 2.45
Phyllostomus elongatus	2	Omnivore	Medium	78.81 ± 21.42	15.05 ± 1.16	7.99 ± 0.56	2.04 ± 0.41
Phyllostomus hastatus	2	Omnivore	Very Hard	142.71 ± 19.45	24.09 ± 6.64	10.77 ± 1.52	7.03 ± 5.03
Sphaeronycteris toxophyllum	1	Frugivore	Very Hard	22.41	1.83	2.89	0.88
Sturnira lilium	2	Frugivore	Hard	32.16 ± 4.08	5.41 ± 0.05	5.69 ± 0.56	1.88 ± 0.36
Tonatia saurophila	3	Insectivore	Medium	71.91 ± 4.31	12.48 ± 2.23	6.44 ± 3.73	2.8 ± 0.66
Trachops cirrhosus	4	Carnivore	Very Hard	69.08 ± 3.41	8.24 ± 1.9	6.87 ± 2	4.2 ± 1.46
Uroderma bilobatum	2	Frugivore	Hard	26.78 ± 5.03	4.74 ± 0.62	4.53 ± 0.3	1.65 ± 0.48
Vampyressa pusilla	1	Frugivore	Hard	12.53	1.08	4.14	0.97

Table S3: Moments about the temporomandibular joint (in N•mm) for each cranial muscle, and out levers (in mm) at the canine and molars for the species under study. Data presented are means ± standard deviations.

Species	n	Moments about the TMJ (N·mm)				Canine Out lever (mm)	Molar Out lever (mm)
		Temporalis	Masseter	Medial pterygoid	Lateral pterygoid		
Anoura geoffroyi	1	6.52	1.05	1.65	0.18	15.69	9.96
Artibeus jamaicensis	2	39.35 ± 1.38	6.6 ± 1.75	5.33 ± 0.54	0.64 ± 0.39	16.3 ± 0.44	10.49 ± 0.02
Carollia brevicauda	4	12.68 ± 2.09	2.92 ± 0.72	2.2 ± 0.35	0.37 ± 0.12	12.62 ± 0.08	8.42 ± 0.09
Carollia perspicillata	2	10.11 ± 0.95	2.71 ± 0.42	2.18 ± 0.47	0.36 ± 0.03	12.8 ± 0.16	8.54 ± 0.02
Centurio senex	1	30.16	2.16	1.08	0.93	8.19	4.91
Desmodus rotundus	1	16.72	3.06	4.68	0.48	10.93	8.57
Enchistenes hartii	2	9.08 ± 2.74	1.39 ± 0.27	1.51 ± 0.16	0.24 ± 0.16	11.32 ± 0.19	7.71 ± 0.02
Glossophaga soricina	1	18.62	1.23	1.21	0.08	12.13	7.77
Lonchophylla robusta	2	8.97 ± 1.61	1.84 ± 0.15	1.86 ± 0.52	0.32 ± 0.19	16.54 ± 0.21	10.4 ± 0.1
Lophostoma brasiliense	3	14.08 ± 4.03	2.95 ± 0.32	1.63 ± 0.26	0.2 ± 0.1	11.24 ± 0.26	7.1 ± 0.09
Lophostoma silvicolum	2	40.21 ± 5.64	8.07 ± 2.62	3.94 ± 1.72	0.85 ± 0.38	15.22 ± 0.55	9.85 ± 0.29
Micronycteris hirsuta	3	18.38 ± 0.63	3.63 ± 0.8	1.66 ± 0.21	0.45 ± 0.13	14.42 ± 0.33	8.87 ± 0.27
Micronycteris megalotis	2	4.49 ± 1.04	1.14 ± 0.13	0.76 ± 0.35	0.08 ± 0.08	10.13 ± 0.27	6.51 ± 0.08
Micronycteris minuta	1	4.11	0.79	0.57	0.09	10.34	6.69
Mimon crenulatum	3	13.36 ± 3.5	2.53 ± 1.14	1.75 ± 0.64	0.44 ± 0.34	12.7 ± 0.55	8.7 ± 0.45
Noctilio albiventris	2	36.28 ± 6.93	2.28 ± 0.34	2.39 ± 0.08	0.9 ± 0.23	12.07 ± 0.44	8.81 ± 0.25
Phylloderma stenops	2	37.01 ± 0.43	9.81 ± 0.73	5.51 ± 0.35	1.29 ± 0.5	18.11 ± 0.35	11.98 ± 0.11
Phyllostomus elongatus	2	40.39 ± 13.44	9.36 ± 0.42	4.58 ± 0.28	0.42 ± 0.07	16.92 ± 0.37	11.23 ± 0.08
Phyllostomus hastatus	2	112.22 ± 24.37	18.8 ± 5.77	9.37 ± 1.95	3.08 ± 2.27	23.59 ± 0.56	15.26 ± 0.32
Sphaeronycteris toxophyllum	1	8.6	0.53	0.76	0.12	7.73	4.9
Sturnira lilium	2	13.49 ± 1.3	2.39 ± 0.12	3.07 ± 0.17	0.51 ± 0.08	12.09 ± 0.2	8.3 ± 0.08
Tonatia saurophila	3	43.77 ± 2.96	7.59 ± 1.24	4.11 ± 2.35	1.16 ± 0.44	16.47 ± 0.24	10.66 ± 0.19
Trachops cirrhosus	4	37.97 ± 1.16	4.58 ± 1.1	4.18 ± 1.42	1.43 ± 0.51	16.41 ± 0.42	11.14 ± 0.4
Uroderma bilobatum	2	12.73 ± 3.96	2.01 ± 0.11	1.9 ± 0.15	0.47 ± 0.14	13 ± 0.23	8.53 ± 0.16
Vampyressa pusilla	1	4.75	0.33	1.28	0.15	9.54	6.19

Table S4: Bite forces (in Newtons) predicted by the uniform traction method and *in vivo* bite forces measured in the field for the 25 species under study. Data presented are means ± standard deviations.

Species	N predicted	Predicted Canine bilateral bite force (N)	Predicted Molar bilateral bite force (N)	N measured	Measured Canine bilateral bite force (N)	Measured Molar bilateral bite force (N)
Anoura geoffroyi	1	1.2	1.89	1	0.22	1.48
Artibeus jamaicensis	2	6.37 ± 0.1	9.9 ± 0.12	152	10.63 ± 3.72	14.17 ± 4.34
Carollia brevicauda	4	2.88 ± 0.39	4.31 ± 0.61	28	6.22 ± 3.45	8.53 ± 3.38
Carollia perspicillata	2	2.4 ± 0.26	3.6 ± 0.45	59	5.76 ± 2.46	7.93 ± 2.71
Centurio senex	1	8.39	14	26	7.85 ± 1.45	10.91 ± 3.04
Desmodus rotundus	1	4.56	5.82	4	2.9 ± 1.5	6.06 ± 0.37
Enchistenes hartii	2	2.16 ± 0.47	3.17 ± 0.65	3	6.07 ± 1	6.21 ± 0.54
Glossophaga soricina	1	3.48	5.44	6	1.29 ± 0.91	1.37 ± 0.7
Lonchophylla robusta	2	1.57 ± 0.2	2.5 ± 0.32	3	3.03 ± 0.84	5.63 ± 2.59
Lophostoma brasiliense	3	3.35 ± 0.62	5.31 ± 1.02	3	7.07 ± 0.11	8.98 ± 0.61
Lophostoma silvicolum	2	6.96 ± 1.11	10.75 ± 1.78	8	12.49 ± 5.02	15.1 ± 4.11
Micronycteris hirsuta	3	3.35 ± 0.06	5.44 ± 0.11	3	7.47 ± 1.92	12.48 ± 3.6
Micronycteris megalotis	2	1.28 ± 0.28	1.99 ± 0.47	4	1.7 ± 0.94	2.31 ± 0.69
Micronycteris minuta	1	1.08	1.66	2	1.77 ± 1.37	3.88 ± 0.1
Mimon crenulatum	3	2.85 ± 0.32	4.17 ± 0.52	6	3.45 ± 0.83	5.66 ± 0.67
Noctilio albiventris	2	6.92 ± 0.81	9.48 ± 1.19	3	5.25 ± 2.13	6.99 ± 2.6
Phylloderma stenops	2	5.92 ± 0.05	8.95 ± 0.01	3	9.73 ± 3.82	15.53 ± 5.72
Phyllostomus elongatus	2	6.45 ± 1.52	9.76 ± 2.58	8	6.04 ± 4.28	11.79 ± 5.64
Phyllostomus hastatus	2	12.14 ± 2.24	18.77 ± 3.51	20	17.24 ± 5.41	23.22 ± 6.1
Sphaeronycteris toxophyllum	1	2.59	4.09	1	2.3	3.77
Sturnira lilium	2	3.22 ± 0.14	4.69 ± 0.24	12	5.72 ± 2.79	8.05 ± 3.74
Tonatia saurophila	3	6.88 ± 0.89	10.64 ± 1.4	8	7.28 ± 2.77	15.41 ± 5.62
Trachops cirrhosus	4	5.87 ± 0.21	8.66 ± 0.35	11	8.01 ± 2.61	11.74 ± 4.67
Uroderma bilobatum	2	2.63 ± 0.59	4 ± 0.89	14	3.55 ± 1.5	4.38 ± 1.57
Vampyressa pusilla	1	1.36	2.1	1	3.53	3.41